

UDC 539.6

## ANALYSIS OF STABILITY AND VIBRATIONS OF POROUS POWER AND SIGMOID FUNCTIONALLY GRADED SANDWICH PLATES BY THE R-FUNCTIONS METHOD

**Lidiya V. Kurpa**

[kurpalidia@gmail.com](mailto:kurpalidia@gmail.com),

ORCID: 0000-0002-4459-8249

**Tetyana V. Shmatko**

[ktv\\_ua@yahoo.com](mailto:ktv_ua@yahoo.com),

ORCID: 0000-0003-3386-8343

**Anna B. Linnik**

[linnik2105@gmail.com](mailto:linnik2105@gmail.com),

ORCID: 0000-0003-4227-3210

National Technical University

"Kharkiv Polytechnic Institute"

2, Kyrpychova str., Kharkiv, 61002, Ukraine

*In this paper, the R-functions method is used for the first time to study the stability and vibrations of porous functionally graded (FG) sandwich plates with a complex geometric shape. It is assumed that the face layers of the plate are made of functionally graded materials, and the middle layer is isotropic, namely ceramic. Differential equations of motion were obtained using the first-order shear deformation theory with a given shear coefficient (FSDT). Two models of porosity distribution according to the power (P-law) and sigmoid (S-law) laws were studied. Analytical expressions for calculating the effective mechanical characteristics of functionally graded materials with even and uneven porosity distribution were obtained. Proposed approach takes into account the fact that the subcritical state of the plate can be heterogeneous, and therefore, first of all, the stresses in the middle plane of the plate are determined, and then the eigenvalue problem is solved in order to find the critical load. To determine the critical load and plate frequencies, the Ritz method combined with the R-functions theory was used. Developed algorithms and software are tested on case studies and compared with known results obtained by another methods. A number of problems of stability and vibrations of the porous functionally graded sandwich plates with a complex geometric shape for various layer arrangement schemes, various boundary conditions and laws of porosity distribution have been solved.*

**Keywords:** stability, vibrations, sandwich plates, porosity, functionally graded material, R-functions method, Ritz method.

### Introduction and analysis of recent research

The tasks of determining the critical load and investigation of free vibrations of plates and shells have always been relevant for engineers engaged in the design of thin-walled structures. It is connected with the requirement to the strength of the structure. Considering that a large number of elements of thin-walled structures are made from functionally graded materials (FGM), this problem is still actual for modern composite materials. Despite a lot of number of foreign papers devoted to this problem [1–3], there are many points that have not solved yet. One of them is the development of effective methods of researching the static and dynamic behavior of functionally graded (FG) plates and shells of complex geometric shape under different types of load and conditions of elements fixed. This especially applies to sandwich FG plates and shells, taking into account such factors as porosity, the presence of an elastic base, uneven load of the object in the middle plane, variable thickness, etc.

Analysis of the existing literature shows that analytical methods for studying the stability and vibrations of elements of rectangular shape that usually are simply supported on the boundary are the most developed ones [4–10]. In the case of plates of a different shape, it is suggested applying the most commonly used numerical finite element method (FEM) [11]. Unfortunately, the authors are not aware of papers in which specific numerical calculations, obtained by FEM for sandwich FG plates of a complex geometric shape (which differ from rectangular plates) taking into account the heterogeneous subcritical state are given.

This paper proposes a numerically analytical approach to solving one of the listed problems, namely, a method for determining the critical load and natural frequencies of porous plates of arbitrary geometric shape. It is assumed that porosity is modeled by power or sigmoid laws. The method is based on the use of

---

This work is licensed under a Creative Commons Attribution 4.0 International License.

© Lidiya V. Kurpa, Tetyana V. Shmatko, Anna B. Linnik, 2023

the R-functions method and the Ritz variational method. The main idea of the method was proposed earlier in papers [12–16] for studying the stability and vibrations of isotropic, orthotropic, single-layer and multi-layer plates, functionally graded single-layer and sandwich plates. In the proposed study, this method was applied for the first time to porous P- and S-FGM sandwich plates. Analytical expressions for calculating the effective properties of such materials were obtained and their reliability was checked on test examples. The developed approach is applied to the calculation of porous FG sandwich plates of complex geometric shape.

**Problem statement**

A porous FG sandwich plate of arbitrary geometric shape compressed by forces in the middle plane is considered. It is assumed that the outer layers are made of FGM, namely from a mixture of metal and ceramics, and the inner layer (core) is ceramic. It is necessary to determine the critical load and natural frequencies of the plate, if there is porosity in the outer layers, and the distribution of partial fractions of ceramics occurs according to different laws, namely, power law and sigmoid law.

**2.1. Mechanical properties of FGM**

Two types of porosity distribution in FG layers are considered: even and uneven. The effective mechanical properties of FGM (Young modulus  $E$  and the material density  $\rho$ ) in case of even distribution of porosity are determined by formulas (1) [7–10]:

$$\begin{cases} P^{(1)}(z) = P_m + (P_c - P_m)V^{(1)}(z) - \frac{\alpha}{2}(P_c + P_m), \\ P^{(2)}(z) = P_m + (P_c - P_m)V^{(2)}(z), \\ P^{(3)}(z) = P_m + (P_c - P_m)V^{(3)}(z) - \frac{\alpha}{2}(P_c + P_m). \end{cases} \quad (1)$$

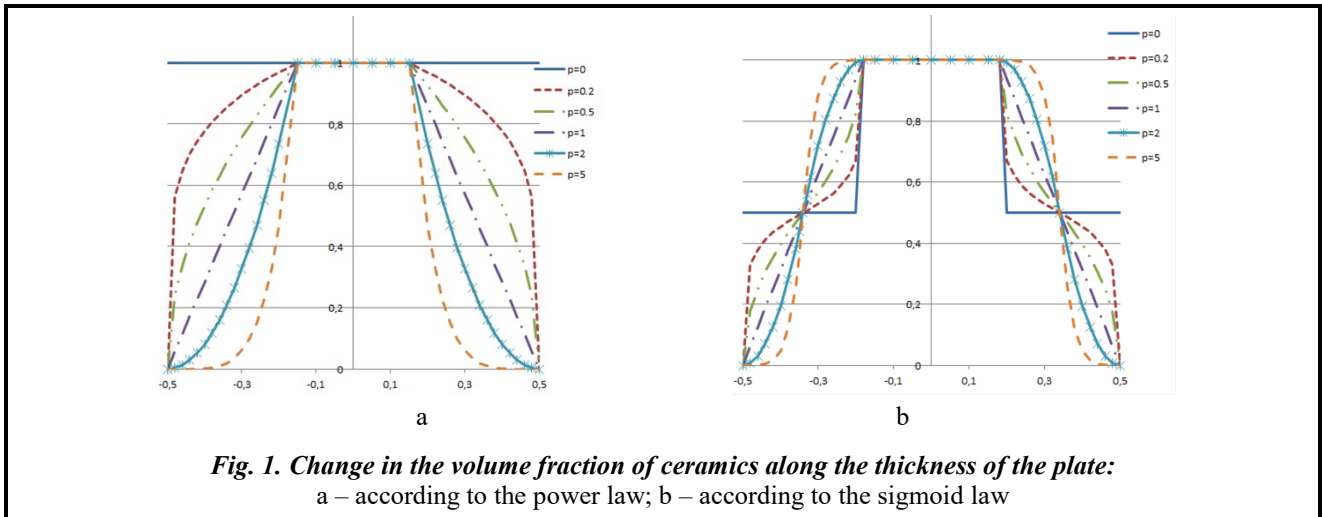
For uneven distribution, they are given by the following expressions:

$$\begin{cases} P^{(1)}(z) = P_m + (P_c - P_m)V^{(1)}(z) - \frac{\alpha}{2}(P_c + P_m) \left( 1 + \frac{z - h_1}{\frac{h}{2} + h_1} \right), \\ P^{(2)}(z) = P_m + (P_c - P_m)V^{(2)}(z), \\ P^{(3)}(z) = P_m + (P_c - P_m)V^{(3)}(z) - \frac{\alpha}{2}(P_c + P_m) \left( \frac{z - \frac{h}{2}}{h_2 - \frac{h}{2}} \right), \end{cases} \quad (2)$$

where  $\alpha$  is the porosity coefficient, and  $V^{(1)}$ ,  $V^{(2)}$ ,  $V^{(3)}$  are partial fractions of ceramics, determined by the corresponding law (Fig. 1, a–b).

For example, for a power law (P-law, Fig. 1, a) they can be determined according to the following formulas [9]:

$$\begin{cases} V^{(1)}(z) = \left( \frac{z + \frac{h}{2}}{h_1 + \frac{h}{2}} \right)^p, & -\frac{h}{2} \leq z \leq h_1, \\ V^{(2)}(z) = 1, & h_1 \leq z \leq h_2, \\ V^{(3)}(z) = \left( \frac{z - \frac{h}{2}}{h_2 - \frac{h}{2}} \right)^p, & h_2 \leq z \leq \frac{h}{2}. \end{cases} \quad (3)$$



**Mathematical formulation of the problem within the framework of the refined first-order shear deformation theory**

To analyze the stability and vibrations of the plate, we use the first-order shear deformation theory [17]. Then displacements  $u, v, w$  at any point of the plate are defined as functions of the displacements of the middle surface  $u_0, v_0$  and  $w_0$  in the directions of the axes  $Ox, Oy$  and  $Oz$  and independent turns  $\psi_x, \psi_y$  of the transverse normal to the middle surface around the axes  $Oy$  and  $Ox$ , respectively:

$$\begin{aligned} u(x, y, z, t) &= u_0(x, y, t) + z\psi_x(x, y, t); \\ v(x, y, z, t) &= v_0(x, y, t) + z\psi_y(x, y, t); \\ w(x, y, z, t) &= w_0(x, y, t). \end{aligned} \tag{4}$$

Components of deformations are defined as

$$\{\varepsilon\} = \{\varepsilon^0\} + z\{\chi^0\},$$

where

$$\{\varepsilon\} = \begin{Bmatrix} \varepsilon_x \\ \varepsilon_y \\ \varepsilon_z \end{Bmatrix}; \{\varepsilon^0\} = \begin{Bmatrix} \frac{\partial u_0}{\partial x} + \frac{1}{2} \left( \frac{\partial w}{\partial x} \right)^2 \\ \frac{\partial v_0}{\partial y} + \frac{1}{2} \left( \frac{\partial w}{\partial x} \right)^2 \\ \frac{\partial u_0}{\partial x} + \frac{\partial v_0}{\partial y} + \frac{1}{2} \left( \frac{\partial w}{\partial x} \right) \left( \frac{\partial w}{\partial y} \right) \end{Bmatrix}; \{\chi^0\} = \begin{Bmatrix} \frac{\partial \varphi_x}{\partial x} \\ \frac{\partial \varphi_x}{\partial y} + \frac{\partial \varphi_y}{\partial x} \end{Bmatrix}; \{\gamma^0\} = \begin{Bmatrix} \gamma_{yz} \\ \gamma_{xz} \end{Bmatrix} = \begin{Bmatrix} \frac{\partial w}{\partial x} + \varphi_x \\ \frac{\partial w}{\partial y} + \varphi_y \end{Bmatrix}.$$

The stresses for each  $r$ -th layer are determined according to Hooke's law as:

$$\{\varepsilon\} = \begin{Bmatrix} \sigma_x \\ \sigma_y \\ \tau_{xy} \\ \tau_{xz} \\ \tau_{yz} \end{Bmatrix} = \begin{bmatrix} Q_{11}(z) & Q_{12}(z) & 0 & 0 & 0 \\ Q_{12}(z) & Q_{22}(z) & 0 & 0 & 0 \\ 0 & 0 & Q_{66}(z) & 0 & 0 \\ 0 & 0 & 0 & Q_{55}(z) & 0 \\ 0 & 0 & 0 & 0 & Q_{44}(z) \end{bmatrix} \cdot \begin{Bmatrix} \varepsilon_x \\ \varepsilon_y \\ \gamma_{xy} \\ \gamma_{xz} \\ \gamma_{yz} \end{Bmatrix},$$

$$Q_{11}(z) = Q_{22}(z) = \frac{E(z)}{1-\nu^2}; Q_{12}(z) = \nu Q_{11}(z); Q_{44}(z) = Q_{55}(z) = Q_{66}(z) = \frac{E(z)}{2(1+\nu)}. \tag{5}$$

Resultant forces in plane  $N=(N_x, N_y, N_{xy})^T$ , moments  $M=(M_x, M_y, M_{xy})^T$  and shear forces  $Q=(Q_x, Q_y)^T$  after integration along the thickness are calculated according to the formulas

$$\{N\} = [A]\{\varepsilon\} + [B]\{\chi\}; \{M\} = [B]\{\varepsilon\} + [D]\{\chi\}; \{Q\} = K_s^2 A_{66} \{\varepsilon_{13}, \varepsilon_{23}\}^T + [B]\{\chi\}, \quad (6)$$

where  $K_s^2$  is the shear correction factor. In this paper, it is taken as  $K_s^2=5/6$ . Note that the elements  $A_{ij}, B_{ij}, D_{ij}$  of the matrices  $[A], [B]$  and  $[D]$  in expressions (6) are calculated by formulas:

$$A_{ij} = \sum_{r=1}^3 \int_{z_r}^{z_{r+1}} Q_{ij}^{(r)} dz; B_{ij} = \sum_{r=1}^3 \int_{z_r}^{z_{r+1}} Q_{ij}^{(r)} z dz; D_{ij} = \sum_{r=1}^3 \int_{z_r}^{z_{r+1}} Q_{ij}^{(r)} z^2 dz,$$

where  $z_1=-h/2; z_2=h_1; z_3=h_2; z_4=h/2$ . Values  $Q_{ij}^{(r)}$  ( $i, j=1, 2, 6$ ) are determined by formulas (5).

Analytical expressions for calculating elements  $A_{ij}, B_{ij}, D_{ij}$  of the matrices  $[A], [B]$  and  $[D]$  are presented for two cases of porosity distribution. For easy and brief presentation the following auxiliary notation was introduced

$$E_{cm} = E_c - E_m; E_{cm}^{(s)} = \alpha \frac{E_c + E_m}{2}; h_c = h_2 - h_1; AS1 = h_1 + \frac{1}{2}h; AS2 = h_2 - \frac{1}{2}h.$$

In this case, the expressions for  $A_{ij}, B_{ij}, D_{ij}$  take the following form:

$$A_{11}^{(1,2)} = \frac{1}{1-\nu^2} (A_{11}^{(g)} - E_{cm}^{(s)} P_{11}^{(1,2)}); B_{11}^{(1,2)} = \frac{1}{1-\nu^2} (B_{11}^{(g)} - E_{cm}^{(s)} P_{12}^{(1,2)}); D_{11}^{(1,2)} = \frac{1}{1-\nu^2} (D_{11}^{(g)} - E_{cm}^{(s)} P_{13}^{(1,2)}).$$

Upper indices correspond to the porosity type: 1 – even distribution; 2 – uneven distribution. Formally, these expressions will be the same for both (P-FGM) and (S-FGM) laws. The expressions for the terms  $A_{11}^{(g)}, B_{11}^{(g)}, D_{11}^{(g)}$  will be different. For the case of the power law (P-FGM), these expressions have the following form:

$$A_{11}^{(g)} = E_m h + E_{cm} \left( \frac{h + p h_c}{p+1} \right); B_{11}^{(g)} = E_{cm} \left( \frac{h_2^2 - h_1^2}{2} + \frac{AS1^2 - AS2^2}{p+2} - \frac{h(AS1 + AS2)}{2(p+1)} \right);$$

$$D_{11}^{(g)} = E_m \frac{h^3}{12} + E_{cm} \left( \frac{AS1^3 - AS2^3}{p+3} - \frac{h(AS1^2 + AS2^2)}{p+2} + \frac{h_2(AS1 + AS2)}{4(p+1)} + \frac{h_2^3 - h_1^3}{3} \right).$$

Expressions for the terms  $P_{11}^{(1,2)}, P_{12}^{(1,2)}, P_{13}^{(1,2)}$  are given below

$$P_{11}^{(1)} = (h - h_c); P_{12}^{(1)} = \left( \frac{h_1^2 - h_2^2}{2} \right); P_{13}^{(1)} = \left( \frac{h^3}{12} - \frac{h_2^3 - h_1^3}{3} \right);$$

$$P_{11}^{(2)} = \frac{1}{2}(h - h_c); P_{12}^{(2)} = \left( \frac{AS1^2 - AS2^2}{3} - \frac{1}{4}h(h_1 + h_2) \right); \quad (7)$$

$$P_{13}^{(2)} = \frac{1}{3} \left( \frac{h^3}{8} + h_1^3 \right) - \frac{AS1^3 + AS2^3}{4} + \frac{2h_1 AS1^2 - h AS2^2}{3} - \frac{1}{2} \left( AS1 h_1^2 + AS2 \frac{h^2}{4} \right).$$

For the sigmoid law (S-FGM) the expressions for  $A_{11}^{(g)}, B_{11}^{(g)}, D_{11}^{(g)}$  have the following form:

$$A_{11}^{(g)} = E_m h + \frac{1}{2} E_{cm} (h + h_c); B_{11}^{(g)} = \frac{1}{2} E_{cm} (h_n^2 - h_m^2) + \frac{AS2^2 - AS1^2}{2(p+1)(p+2)};$$

$$D_{11}^{(g)} = E_m \frac{h^3}{12} + E_{cm} \left( \frac{h_n^3 - h_m^3}{3} + \frac{AS2^2 \left( h_2 + \frac{h}{2} \right) - AS1^2 \left( h_1 - \frac{h}{2} \right)}{4(p+1)(p+2)} \right).$$

Expressions  $P_{11}^{(1,2)}, P_{12}^{(1,2)}, P_{13}^{(1,2)}$  for both P-S-FG laws have the same form (15).

All other elements  $A_{12}, A_{66}, B_{12}, B_{66}, D_{12}, D_{66}$  are defined using the obtained formulas for  $A_{11}, B_{11}, D_{11}$ , namely:

$$\begin{aligned}
 A_{12} &= \nu A_{11}; \quad A_{22} = A_{11}; \quad A_{66} = \frac{1-\nu}{2} A_{11}; \\
 B_{12} &= \nu B_{11}; \quad B_{22} = B_{11}; \quad B_{66} = \frac{1-\nu}{2} B_{11}; \\
 D_{12} &= \nu D_{11}; \quad D_{22} = D_{11}; \quad D_{66} = \frac{1-\nu}{2} D_{11}.
 \end{aligned}$$

We assume that a compressive static load  $p_{st}$  acts on the plate, and all external forces change proportionally to the parameter  $\lambda$ . The main differential equations for the equilibrium of a plate loaded in the middle plane have the following form:

$$\begin{aligned}
 \frac{\partial N_x}{\partial x} + \frac{\partial N_{xy}}{\partial y} - m_1 \frac{\partial^2 u}{\partial t^2} &= 0; \\
 \frac{\partial N_{xy}}{\partial x} + \frac{\partial N_y}{\partial y} - m_1 \frac{\partial^2 v}{\partial t^2} &= 0; \\
 \frac{\partial Q_x}{\partial x} + \frac{\partial Q_y}{\partial y} + \lambda \left( \frac{\partial^2 N_x}{\partial x^2} + 2 \frac{\partial^2 N_{xy}}{\partial x \partial y} + \frac{\partial^2 N_y}{\partial y^2} \right) - m_1 \frac{\partial^2 w}{\partial t^2} &= 0; \\
 \frac{\partial M_x}{\partial x} + \frac{\partial M_y}{\partial y} - Q_x - m_2 \frac{\partial^2 \psi_x}{\partial t^2} &= 0;
 \end{aligned} \tag{8}$$

where  $N_x, N_y, N_{xy}$  are forces that describe the subcritical state of the plate, and  $m_1 = \sum_{s=1}^n \int_{h_s}^{h_{s+1}} \rho_0^{(r)} dz$ ,

$m_2 = \sum_{s=1}^n \int_{h_s}^{h_{s+1}} \rho_0^{(r)} z^2 dz$ ;  $\rho_0^{(s)}$  is the density of the  $r$ -th layer.

Equations of motion (8) are supplemented by appropriate boundary conditions.

**Solution method**

In the general case, the subcritical state of the plate can be heterogeneous. For example, it is regarding to plates with holes, active complex load or plates with a complex geometric shape, etc. So, it is important to determine the subcritical state of the plate first, that is, to find the forces in the middle plane  $\{N^0\} = (N_x^0, N_y^0, N_{xy}^0)^T$ . Considering that the plate keeps the flat form, the values  $w, \psi_x, \psi_y$  can be neglected when finding these forces. Therefore, we will assume that the subcritical state of the plate is modeled by the following system of equations

$$\begin{cases} \frac{\partial N_x}{\partial x} + \frac{\partial N_{xy}}{\partial y} = 0 \\ \frac{\partial N_{xy}}{\partial x} + \frac{\partial N_y}{\partial y} = 0 \end{cases} \tag{9}$$

System (9) is supplemented by the following boundary conditions on the loaded boundary part  $\partial\Omega_1$ :

$$N_n(u, v) = -1; \quad T_n(u, v) = 0. \tag{10}$$

Operators  $N_n, T_n$  are defined as:

$$N_n = N_{11}l^2 + N_{22}m^2 + 2N_{12}lm; \quad T_n = N_{12}(l^2 - m^2) + (N_{11} - N_{22})lm.$$

where  $l = \cos(\vec{n}, Ox)$ ;  $m = \cos(\vec{n}, Oy)$ ; and vector  $\vec{n}$  is the normal vector to the region boundary. The type of boundary conditions on the unloaded part of the area is determined by fixing way.

Problem (9–10) is solved using the Ritz method joined with the R-functions theory [18]. Therefore, we present a variational statement of problem (9–10), which is reduced to finding the extremum of the following functional:

$$I(u_0, v_0) = \frac{1}{2} \int_{\Omega} (N_x^0 \varepsilon_x^L + N_y^0 \varepsilon_y^L + N_{xy}^0 \gamma_{xy}^L) d\Omega + \int_{\partial\Omega_1} p_{st} (u_0 \cos \alpha + v_0 \sin \alpha) ds, \quad (11)$$

where

$$\{N^0\} = [A] \{\varepsilon_0\}^T; \{\varepsilon_0\} = \{u_{0,x}; v_{0,y}; u_{0,y} + v_{0,x}\}.$$

Solution of the boundary value problem (9–10) or the variational problem (11) allows to determine the displacement  $u_0, v_0$ , and therefore the forces  $\{N_0\}$  in the middle plane, which describe the subcritical plate state.

To find the critical load we use the dynamic approach [19], as it was earlier in Ref. [15, 16]. For this, it is necessary to find the extremum of the function:

$$I(u, v, w, \psi_x, \psi_y) = \frac{1}{2} \iint_{\Omega} [N_x^L \varepsilon_x^L + N_y^L \varepsilon_y^L + N_{xy}^L \gamma_{xy}^L + M_x \chi_x + M_y \chi_y + M_{xy} \chi_{xy} + Q_x \varepsilon_{xz} + Q_y \varepsilon_{yz} + p_{st} (N_x^0 (w_{,x})^2 + N_y^0 (w_{,y})^2 + N_{xy}^0 w_{,x} w_{,y})] d\Omega - \frac{1}{2} \omega_L^2 \iint_{\Omega} (I_0 (u^2 + v^2 + w^2) + I_1 (u\varphi_x + v\varphi_y) + I_2 (\psi_x^2 + \psi_y^2)) d\Omega. \quad (12)$$

The value of the parameter  $p_{st}$  will be increased until the frequency  $\omega_L$  will be a real number. The magnitude of the critical load  $N_{cr}$  is determined by the value of the parameter  $p_{st}$ , which corresponds to the smallest non-negative value of the square of frequency. Values  $I_0, I_1, I_2$  in the formula (12) are calculated as the following integrals

$$(I_0, I_1, I_2) = \sum_{r=1}^3 \int_{z_r}^{z_{r+1}} (\rho^{(r)}(1, z, z^2)) dz.$$

Taking into account the fact that the mass density of the  $r$ -th layer is determined by formulas (1–3), analytical expressions for calculating  $I_0, I_1, I_2$  were obtained:

– for a power law (P-law)

$$I_0^{(1,2)} = IA_{11}^g - \rho_{cm}^{(r)} P_{11}^{(1,2)}; I_1^{(1,2)} = IB_{11}^g - \rho_{cm}^{(r)} P_{12}^{(1,2)}; I_2^{(1,2)} = ID_{11}^g - \rho_{cm}^{(r)} P_{13}^{(1,2)}. \quad (13)$$

Expressions for  $IA_{11}^g, IB_{11}^g, ID_{11}^g$  are shown below

$$IA_{11}^g = IA_{11}^{(gp)}; IB_{11}^g = IB_{11}^{(gp)}; ID_{11}^g = ID_{11}^{(gp)},$$

where  $IA_{11}^{(gp)} = \rho_m h + \rho_{cm} \left( \frac{h + ph_c}{p+1} \right); IB_{11}^{(gp)} = \rho_{cm} \left( \frac{h_2^2 - h_1^2}{2} + \frac{AS1^2 - AS2^2}{p+2} - \frac{h(AS1 + AS2)}{2(p+1)} \right);$

$$ID_{11}^{(gp)} = \rho_m \frac{h^3}{12} + \rho_{cm} \left( \frac{h_2^3 - h_1^3}{3} + \frac{AS1^3 - AS2^3}{p+3} - \frac{h(AS1^2 + AS2^2)}{p+2} + \frac{h_2(AS1 - AS2)}{4(p+1)} \right).$$

– for a sigmoid law (S-law)

$$IA_{11}^g = IA_{11}^{(gs)}; IB_{11}^g = IB_{11}^{(gs)}; ID_{11}^g = ID_{11}^{(gs)},$$

where  $IA_{11}^{(gs)}, IB_{11}^{(gs)}, ID_{11}^{(gs)}$  are defined as:

$$IA_{11}^{(gs)} = \rho_m h + \frac{1}{2} \rho_{cm} (h + h_c); IB_{11}^{(gs)} = \frac{1}{2} \rho_{cm} (h_2^2 - h_1^2) + \frac{AS2^2 - AS1^2}{2(p+1)(p+2)};$$

$$ID_{11}^{(gs)} = \rho_m \frac{h^3}{12} + \rho_{cm} \left( \frac{h_n^3 - h_m^3}{3} + \frac{AS2 \left( h_2 + \frac{h}{2} \right) - AS1 \left( h_1 - \frac{h}{2} \right)}{4(p+1)(p+2)} \right).$$

Expressions for  $P_{11}^{(1,2)}$ ,  $P_{12}^{(1,2)}$ ,  $P_{13}^{(1,2)}$  in formulas (13) have the form (7).

Finding the stationary point of the functional (12) is performed by the Ritz method. The sequence of coordinate functions was constructed using the R-functions method [18].

**Numerical results**

**Test tasks**

The presented algorithm was tested for the following examples. Let's assume that simply supported FG square sandwich plate compressed by forces uniformly along all the sides. The outer layers are made of FGM Al/Al<sub>2</sub>O<sub>3</sub>, and the core is metal. Layer thicknesses and gradient index  $p$  vary. The ratio of the total thickness of the plate  $h$  to the length of the side of the square  $2a$  is taken 0.1, i.e.  $h/(2a)=0.1$ . Properties of both materials for FGM mixture Al/Al<sub>2</sub>O<sub>3</sub> are as follows [9, 17]: Al –  $E_m=70$  GPa;  $\nu_m=0.3$ ;  $\rho_m=2707$  kg/m<sup>3</sup>; Al<sub>2</sub>O<sub>3</sub> –  $E_c=380$  GPa;  $\nu_c=0.3$ ;  $\rho_c=3800$  kg/m<sup>3</sup>.

A similar problem was considered in paper [10]. Table 1 shows a comparison of the obtained results for a dimensionless critical load  $\bar{N}_{cr} = \frac{N_{cr}}{100E_0h^3}$  (where  $E_0=1$  GPa;  $\rho_0=1$  kg/m<sup>3</sup>) with the results of paper [10] for FGM Al<sub>2</sub>O<sub>3</sub>/Al,  $p=2$ . Various layers arrangement schemes are considered  $h^{(1)}-h^{(2)}-h^{(3)}$ . Values  $h^{(1)}$ ,  $h^{(2)}$ ,  $h^{(3)}$  determine the thickness of the layers and are equal to  $h^{(1)}=h_1+h/2$ ;  $h^{(2)}=h_2-h_1$ ;  $h^{(3)}=h/2-h_2$ .

Table 2 shows a comparison of the obtained results for the natural frequency  $\Lambda = \frac{\lambda(2a)^2}{h} \sqrt{\frac{\rho_0}{E_0}}$  of simply supported plate with outer layers made of FGM (Al<sub>2</sub>O<sub>3</sub>/Al,  $p=2$ ), with similar results of the paper [10].

**Table 1. Comparison of the critical load with known results for a square simply supported plate compressed along the whole boundary by uniform forces (Al<sub>2</sub>O<sub>3</sub>/Al,  $p=2$ )**

Porosity type	$\alpha$	Method	1-0-1	1-1-1	1-2-1	2-1-2
P-FGM	0	[10]	1.7786	2.4045	2.9934	2.0828
		RFM	1.7681	2.3920	2.9830	2.0715
P-I (even)	0.1	[10]	1.3623	1.9972	2.6223	1.6648
		RFM	1.3783	2.1980	2.0647	1.6850
	0.2	[10]	0.9303	1.6046	2.2654	1.2621
		RFM	0.9870	1.6451	2.3072	1.2573
P-II (uneven)	0.1	[10]	1.6660	2.2576	2.8409	1.9485
		RFM	1.6686	2.2633	2.8501	1.9515
	0.2	[10]	1.5633	2.1134	2.6927	1.8181
		RFM	1.5695	2.1335	2.7181	1.8325
S-FGM	0	[10]	2.2554	3.0372	3.6296	2.6673
		RFM	2.2441	3.0265	3.6219	2.6560
S-I (even)	0.1	[10]	1.8310	2.6215	3.2501	2.2416
		RFM	1.8541	2.6381	3.2325	2.2681
	0.2	[10]	1.4224	2.2216	2.8861	1.8323
		RFM	1.4565	2.2496	2.8451	1.8772
S-II (uneven)	0.1	[10]	2.1429	2.8844	3.4716	2.5287
		RFM	2.1465	2.8962	3.4882	2.5365
	0.2	[10]	2.0326	2.7359	3.3184	2.3937
		RFM	2.0462	2.7675	3.3561	2.4182

**Table 2. Comparison of the dimensionless parameter of the natural frequency of a square simply supported sandwich FG plate with known results,  $p=2$ ,  $p=2$ ,  $h/(2a)=0,1$**

$\alpha$	Method	1-0-1	1-1-1	1-2-1	2-1-2	2-2-1	2-1-1
P-I, FGM							
0	[10]	1.0615	1.1885	1.3024	1.1225	1.2439	1.1653
	RFM	1.0584	1.1857	1.3002	1.1195	1.2415	1.1627
0.1	[10]	0.9826	1.1207	1.2493	1.0471	1.1819	1.0935
	RFM	0.9885	1.1271	1.2549	1.0531	1.1880	1.1007
0.2	[10]	0.8787	1.0420	1.1915	1.9549	1.1105	1.0056
	RFM	0.8913	1.0551	1.2026	0.9684	1.1228	1.0188
P-II, FGM							
0.1	[10]	1.0556	1.1708	1.2842	1.1084	1.2270	1.1512
	RFM	1.0565	1.1725	1.2864	1.0941	1.2277	1.1512
0.2	[10]	1.0521	1.1526	1.2658	1.0939	1.2097	1.1376
	RFM	1.0544	1.1581	1.2717	1.0984	1.2126	1.1383
S-I, FGM							
0	[10]	1.1617	1.3119	1.4155	1.2427	1.3594	1.2797
	RFM	1.1588	1.3096	1.4137	1.2401	1.3573	1.2774
0.1	[10]	1.1039	1.2595	1.3718	1.1862	1.3113	1.2262
	RFM	1.1105	1.2676	1.3792	1.1942	1.3189	1.2339
0.2	[10]	1.0315	1.2011	1.3256	1.2076	1.2580	1.1632
	RFM	1.0467	1.2173	1.3399	1.1371	1.2732	1.1797
S-II, FGM							
0.1	[10]	1.1615	1.2992	1.4001	1.2340	1.3470	1.2712
	RFM	1.1641	1.3029	1.4046	1.2374	1.3502	1.2740
0.2	[10]	1.1620	1.2864	1.3859	1.2255	1.3346	1.2628

**Stability and free vibrations of plates with a complex geometric shape**

Comparison of data in the Tables 1 and 2 indicates a good agreement between the obtained results and those known in the literature. This fact allows to consider plates with a complex geometric shape with cutouts, as shown in Figs. 4 and 5.

The geometric parameters are taken as follows:  $b/2a=0.75$ ;  $a_1/2a=0.35$ ;  $b_1/2a=0.15$ ;  $R/2a=0.2$ ;  $h/2a=0.1$ .

The equation of the boundary of this region  $\omega(x, y)=0$  is constructed using the R-functions method, where

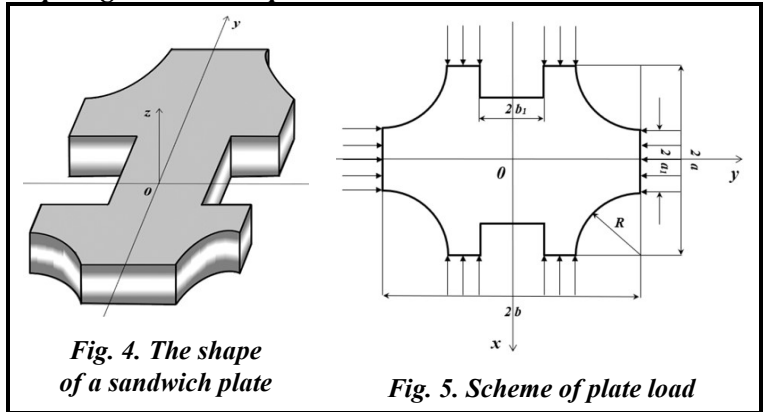


**Fig. 4. The shape of a sandwich plate**

**Fig. 5. Scheme of plate load**

$$\omega(x, y) = (f_1 \wedge_0 f_2) \wedge_0 (f_3 \wedge_0 f_4) \wedge_0 (f_5 \wedge_0 f_6) \wedge_0 (f_7 \wedge_0 f_8). \tag{14}$$

Functions  $f_i(x, y)$ , ( $i = \overline{1,8}$ ) in expression (14) are determined by the following inequalities:

$$f_1 = \frac{a^2 - x^2}{2a} \geq 0; f_2 = \frac{b^2 - y^2}{2b} \geq 0; f_3 = \frac{a_1^2 - x^2}{2a_1} \geq 0; f_4 = \frac{y^2 - b_1^2}{2b_1} \geq 0; f_5 = \frac{R^2 - (x-a)^2 - (y-b)^2}{2R} \geq 0;$$

$$f_6 = \frac{R^2 - (x+a)^2 - (y-b)^2}{2R} \geq 0; f_7 = \frac{R^2 - (x-a)^2 - (y+b)^2}{2R} \geq 0; f_8 = \frac{R^2 - (x+a)^2 - (y+b)^2}{2R} \geq 0,$$

where operations  $\wedge_0, \vee_0$  have the following type:  $f_k \wedge_0 f_s = f_k + f_s - \sqrt{f_k^2 + f_s^2}$  is the R-conjunction that describes the intersection of regions defined by analytic inequalities  $f_k \geq 0, f_s \geq 0$ ;  $f_k \vee_0 f_s \equiv f_k + f_s + \sqrt{f_k^2 + f_s^2}$  is the R-disjunction that describes the union of areas defined by analytical inequalities  $f_k \geq 0, f_s \geq 0$ .

Two types of boundary conditions are considered:

– BC-I – plate that is clamped along the sides  $x=\pm a, y=\pm b$ , that is, on the parts of the border where compressive forces are acting, the remaining part is free;

– BC-II – plate that is clamped along the whole contour.

Table 3 shows the value of the critical load

$$\bar{N}_{cr} = \frac{N_{cr}}{100E_0h^3}$$

for different laws of porosity distribution at a fixed value of the volume fraction of ceramics  $p=2$ .

Figs. 6, a–b show the influence of the gradient index on the natural frequencies of vibrations of sandwich plates for different schemes of the layers arrangement with even and uneven distribution of porosity, when the value of the porosity coefficient is  $\alpha=0.1$ .

Comparing Figs. 6, a and 6, b, the following conclusions can be drawn: in both cases, when the gradient index increases, the frequencies decrease. Starting with  $p=5$ , the decrease is quite smooth, that is, the influence of the gradient index will be insignificant; the highest values of frequencies have the plates in the case of the 1-2-1 scheme, both with even and uneven distribution of porosity, which has a good agreement aligns well with the physical sense content. In this case, the content volume of ceramics will be the greatest, and the plate will be the most rigid. For the sigmoid law (Fig. 6, b), the layers thicknesses have a more significant effect on the frequencies than for the power law (Fig. 6, a).

**Table 3. Critical load for a porous plate of a complex geometric shape**

*with boundary conditions BC-I,  $p=2$ ;  $Al/Al_2O_3$*

Law	$\alpha$	1-0-1	1-1-1	1-2-1	2-1-2
P-I	0	4.6550	6.3150	7.8356	5.469
	0.1	3.6450	5.3540	6.9785	4.474
	0.2	2.6330	4.3840	6.1112	3.465
P-II	0.1	4.3935	5.9800	7.4950	5.162
	0.2	4.1315	5.6420	7.1550	4.847
S-I	0	5.9157	7.9440	9.4580	6.990
	0.1	4.9095	6.9470	8.6050	6.002
	0.2	3.8959	6.0385	7.7530	5.005
S-II	0.1	5.6702	7.6111	9.1221	6.681
	0.2	5.3928	7.2755	8.7850	6.371



Fig. 7 presents graphs of frequency behavior for plates that are clamped along the whole contour for two laws of volume fraction distribution of P-FGM and S-FGM ceramics, provided there is no porosity,  $\alpha=0$ .

The effect of the porosity coefficient on the natural frequencies of such plates for the arrangement of layers (1-1-1) is shown in Fig. 8. As can be seen, the change in the porosity coefficient within the selected interval  $0 \leq \alpha \leq 0.2$  has almost no effect on the behavior of the clamped plate for both sigmoid and power laws. For the power law, this influence is more considerable, although it is also insignificant.

Figs. 9, a–b show the graphs of frequency behavior for porous plates that are clamped along the whole contour (BC-II) with uneven porosity distribution for two P-FGM and S-FGM laws of changes in the volume fraction of ceramics: a –  $\alpha=0.1$ ; b –  $\alpha=0.2$ . Various layers arrangement schemes are considered: 1-0-1; 1-1-1; 1-2-1; 2-1-2.

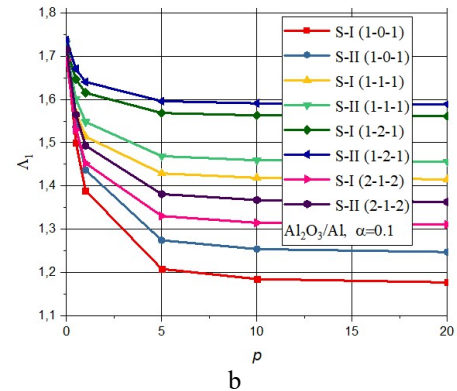
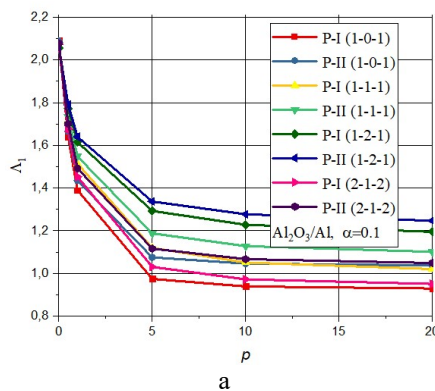


Fig. 6. Natural frequencies of a porous sandwich plate, BC-I: a – P-FGM; b – S-FGM

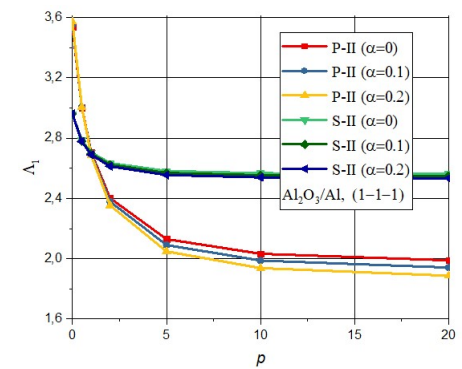
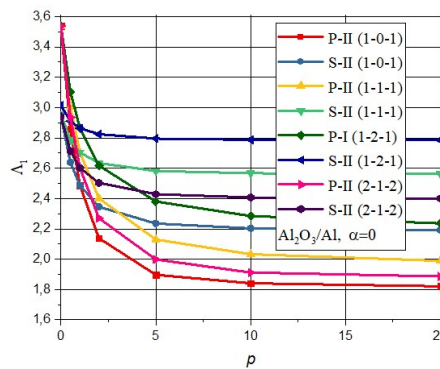


Fig. 7. Natural frequencies of the plate clamped along the whole contour (P-FGM and S-FGM) without porosity

Fig. 8. The effect of the porosity coefficient on the natural frequencies (P-FGM and S-FGM) of the plate for the scheme (1-1-1)

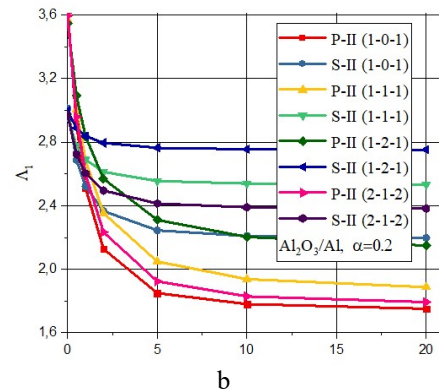
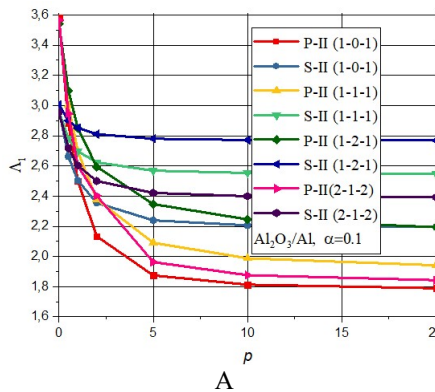


Fig. 9. Natural frequencies of a porous sandwich plate clamped along the whole contour (BC-II): a –  $\alpha=0.1$ ; b –  $\alpha=0.2$

It can be seen from the given graphs that the frequencies have greater values with the sigmoidal law of change of the effective properties of the material for all considered schemes of thickness values. The gradient index values from 0 to 5 have the most significant effect on the reduction of natural frequencies. Changing the porosity parameter does not significantly affect the frequency values. This can be observed more clearly from the graph in Fig. 8.

### Prospects for further research

From the point of authors' view, the further studies of the considered topic can be devoted to the development of the proposed methods using the higher order shear deformation theory.

### Conclusions

An numerically analytical approach for studying the stability and vibrations of porous FG plates, which is based on the use of the R-functions method and variational methods, is proposed.

It is shown and confirmed by examples that the developed method allows to study the FG porous sandwich plates taking into account the heterogeneous subcritical state and complex geometric shape.

The influence of the gradient index and different porosity distribution laws (P-FGM and S-FGM) on natural frequencies and critical load was studied.

Analytical expressions for calculating the effective properties of FGM for even and uneven porosity distribution for sigmoid and power laws were obtained.

The stability and vibrations of a plate with a complex geometric form compressed by forces in the middle plane were analyzed.

### References

1. Thai, H.-T. & Kim, S.-E. (2015). A review of theories for the modeling and analysis of functionally graded plates and shells. *Composite Structures*, vol. 128, pp. 70–86. <https://doi.org/10.1016/j.compstruct.2015.03.010>.
2. Swaminathan, K., Naveenkumar, D. T., Zenkour, A. M., & Carrera, E. (2015). Stress, vibration and buckling analyses of FGV plates – A state-of-the-art review. *Composite Structures*, vol. 120, pp. 10–31. <https://doi.org/10.1016/j.compstruct.2014.09.070>.
3. Kumar, Y. (2017). The Rayleigh–Ritz method for linear dynamic, static and buckling behavior of beams, shells and plates: A literature review. *Journal of Vibration and Control*, vol. 24, iss. 7, pp. 1205–1227. <https://doi.org/10.1177/1077546317694724>.
4. Elmeiche, N., Tounsi, A., Ziane, N., Mechab, I., & El Abbes, A. B. (2011). A new hyperbolic shear deformation theory for buckling and vibration of functionally graded sandwich plate. *International Journal of Mechanical Sciences*, vol. 53, iss. 4, pp. 237–247. <https://doi.org/10.1016/j.ijmecsci.2011.01.004>.
5. Neves, A. M. A., Ferreira, A. J. M., Carrera, E., Cinefra, M., Jorge, R. M. N., & Soares, C. M. M. (2012). Buckling analysis of sandwich plates with functionally graded skins using a new quasi-3D hyperbolic sine shear deformation theory and collocation with radial basis functions. *Journal of Applied Mathematics and Mechanics*, vol. 92, iss. 9, pp. 749–766. <https://doi.org/10.1002/zamm.201100186>.
6. Yaghoobi, H. & Yaghoobi, P. (2013). Buckling analysis of sandwich plates with FGM face sheets resting on elastic foundation with various boundary conditions: An analytical approach. *Meccanica*, vol. 48, pp. 2019–2035. <https://doi.org/10.1007/s11012-013-9720-0>.
7. Singh, S. J. & Harsha, S. P. (2019). Exact solution for free vibration and buckling of sandwich S-FGM plates on Pasternak elastic foundation with various boundary conditions. *International Journal of Structural Stability and Dynamics*, vol. 19, no. 3, paper 1950028. <https://doi.org/10.1142/S0219455419500287>.
8. Li, D., Zhu, H., & Gong, X. (2021). Buckling analysis of functionally graded sandwich plates under both mechanical and thermal loads. *Materials*, vol. 14, iss. 23, paper 7194. <https://doi.org/10.3390/ma14237194>.
9. Zencour, A. M. (2005). A comprehensive analysis of functionally graded sandwich plates: Part 2 – Buckling and free vibration. *International Journal of Solids and Structures*, vol. 42, iss. 18–19, pp. 5243–5258. <https://doi.org/10.1016/j.ijsolstr.2005.02.016>.
10. Daikh, A. A. & Zenkour, A. M. (2019). Free vibration and buckling of porous power-law and sigmoid functionally graded sandwich plates using a simple higher-order shear deformation theory. *Materials Research Express*, vol. 6, no. 11, paper 115707. <https://doi.org/10.1088/2053-1591/ab48a9>.
11. Le, C. I., Tran, Q. D., Pham, V. N., & Nguyen, D. K. (2021). Free vibration and buckling of bidirectional functionally graded sandwich plates using an efficient Q9 element. *Vietnam Journal of Mechanics*, vol. 43, no. 3, pp. 277–295. <https://doi.org/10.15625/0866-7136/15981>.
12. Kurpa, L., Mazur, O., & Tkachenko, V. (2013). Dynamical stability and parametrical vibrations of the laminated plates with complex shape. *Latin American Journal of Solids and Structures*, vol. 10, iss. 1, pp. 175–188. <https://doi.org/10.1590/S1679-78252013000100017>.
13. Awrejcewicz, J., Kurpa, L., & Mazur, O. (2016). Dynamical instability of laminated plates with external cutout. *International Journal of Non-Linear Mechanics*, vol. 81, pp. 103–114. <https://doi.org/10.1016/j.ijnonlinmec.2016.01.002>.

14. Awrejcewicz, J., Kurpa, L., & Shmatko, T. (2017). Analysis of geometrically nonlinear vibrations of functionally graded shallow shells of a complex shape. *Latin American Journal of Solids and Structures*, vol. 14, iss. 9, pp. 1648–1668. <https://doi.org/10.1590/1679-78253817>.
15. Kurpa, L. V. & Shmatko, T. V. (2020). Investigation of free vibrations and stability of functionally graded three-layer plates by using the R-functions theory and variational methods. *Journal of Mathematical Sciences*, vol. 249, no. 3, pp. 496–520. <https://doi.org/10.1007/s10958-020-04955-2>.
16. Kurpa, L. V. & Shmatko, T. V. (2020). Buckling and free vibration analysis of functionally graded sandwich plates and shallow shells by the Ritz method and the R-functions theory. *Proceedings of the Institution of Mechanical Engineers, Part C: Journal of Mechanical Engineering Science*, vol. 235, iss. 20, pp. 4582–4593. <https://doi.org/10.1177/0954406220936304>.
17. Shen, H.-S. (2011). *Functionally graded materials. Nonlinear analysis of plates and shells*. USA, Boca Raton: CRC Press, 280 p. <https://doi.org/10.1201/9781420092578>.
18. Rvachev, V. L. (1982). *Teoriya R-funktsiy i nekotoryye yeye prilozheniya* [The R-functions theory and some of its applications]. Kyiv: Naukova dumka, 552 p. (in Russian).
19. Lekhnitskiy, S. G. (1957). *Anizotropnyye plastinki* [Anisotropic plates]. Moscow: Gostekhizdat, 464 p. (in Russian).

*Received 08 August 2023*

### **Аналіз стійкості та коливань пористих степеневих та сигмовидних функціонально-градієнтних сендвіч-пластин методом R-функцій**

**Л. В. Курпа, Т. В. Шматко, Г. Б. Лінник**

Національний технічний університет «Харківський політехнічний інститут»  
61002, Україна, м. Харків, вул. Кирпичова, 2

*У даній роботі вперше застосовано метод R-функцій для дослідження стійкості та коливань пористих функціонально-градієнтних сендвіч-пластин зі складною геометричною формою. Припускається, що зовнішні шари пластини виготовлено із функціонально-градієнтних матеріалів, а заповнювач є ізотропним, а саме керамічним. Диференціальні рівняння руху одержано за допомогою звичайної зсувної деформаційної теорії першого порядку із заданим коефіцієнтом зсуву (FSDT). Досліджено дві моделі розподілення пористості згідно із степеневим (P-law) і сигмовидним (S-law) законами. Одержані аналітичні вирази для обчислення ефективних механічних характеристик функціонально-градієнтних матеріалів при рівномірному й нерівномірному розподіленні пористості. Запропонований підхід враховує той факт, що докритичний стан пластини може бути неоднорідним, і тому перш за все визначаються напруження в серединній площині пластини, а потім розв'язується задача на власні значення з метою знаходження критичного навантаження. Для визначення критичного навантаження і частот пластин використано метод Рітца разом із теорією R-функцій. Розроблені алгоритми і програмне забезпечення перевірені на тестових прикладах і порівняні з відомими результатами, одержаними за допомогою інших методів. Вирішено ряд задач стійкості й коливань пористих функціонально-градієнтних сендвіч-пластин зі складною геометричною формою для різних схем укладання шарів, різних крайових умов і законів розподілення пористості.*

**Ключові слова:** *стійкість, коливання, сендвіч-пластини, пористість, функціонально-градієнтний матеріал, теорія R-функцій, метод Рітца.*

#### **Література**

1. Thai H.-T., Kim S.-E. A review of theories for the modeling and analysis of functionally graded plates and shells. *Composite Structures*. 2015. Vol. 128. P. 70–86. <https://doi.org/10.1016/j.compstruct.2015.03.010>.
2. Swaminathan K., Naveenkumar D. T., Zenkour A. M., Carrera E. Stress, vibration and buckling analyses of FGV plates – A state-of-the-art review. *Composite Structures*. 2015. Vol. 120. P. 10–31. <https://doi.org/10.1016/j.compstruct.2014.09.070>.
3. Kumar Y. The Rayleigh–Ritz method for linear dynamic, static and buckling behavior of beams, shells and plates: A literature review. *Journal of Vibration and Control*. 2017. Vol. 24. Iss. 7. P. 1205–1227. <https://doi.org/10.1177/1077546317694724>.

4. Elmeiche N., Tounsi A., Ziane N., Mechab I., El Abbes A. B. A new hyperbolic shear deformation theory for buckling and vibration of functionally graded sandwich plate. *International Journal of Mechanical Sciences*. 2011. Vol. 53. Iss. 4. P. 237–247. <https://doi.org/10.1016/j.ijmecsci.2011.01.004>.
5. Neves A. M. A., Ferreira A. J. M., Carrera E., Cinefra M., Jorge R. M. N., Soares C. M. M. Buckling analysis of sandwich plates with functionally graded skins using a new quasi-3D hyperbolic sine shear deformation theory and collocation with radial basis functions. *Journal of Applied Mathematics and Mechanics*, 2012. Vol. 92. Iss. 9. P. 749–766. <https://doi.org/10.1002/zamm.201100186>.
6. Yaghoobi H., Yaghoobi P. Buckling analysis of sandwich plates with FGM face sheets resting on elastic foundation with various boundary conditions: An analytical approach. *Meccanica*. 2013. Vol. 48. P. 2019–2035. <https://doi.org/10.1007/s11012-013-9720-0>.
7. Singh S. J., Harsha S. P. Exact solution for free vibration and buckling of sandwich S-FGM plates on Pasternak elastic foundation with various boundary conditions. *International Journal of Structural Stability and Dynamics*. 2019. Vol. 19. No. 3. Paper 1950028. <https://doi.org/10.1142/S0219455419500287>.
8. Li D., Zhu H., Gong X. Buckling analysis of functionally graded sandwich plates under both mechanical and thermal loads. *Materials*. 2021. Vol. 14. Iss. 23. Paper 7194. <https://doi.org/10.3390/ma14237194>.
9. Zencour A. M. A comprehensive analysis of functionally graded sandwich plates: Part 2 – Buckling and free vibration. *International Journal of Solids and Structures*. 2005. Vol. 42. Iss. 18–19. P. 5243–5258. <https://doi.org/10.1016/j.ijsolstr.2005.02.016>.
10. Daikh A. A., Zenkour A. M. Free vibration and buckling of porous power-law and sigmoid functionally graded sandwich plates using a simple higher-order shear deformation theory. *Materials Research Express*. 2019. Vol. 6. No. 11. Paper 115707. <https://doi.org/10.1088/2053-1591/ab48a9>.
11. Le C. I., Tran Q. D., Pham V. N., Nguyen D. K. Free vibration and buckling of bidirectional functionally graded sandwich plates using an efficient Q9 element. *Vietnam Journal of Mechanics*. 2021. Vol. 43. No. 3. P. 277–295. <https://doi.org/10.15625/0866-7136/15981>.
12. Kurpa L., Mazur O., Tkachenko V. Dynamical stability and parametrical vibrations of the laminated plates with complex shape. *Latin American Journal of Solids and Structures*. 2013. Vol. 10. Iss. 1. P. 175–188. <https://doi.org/10.1590/S1679-78252013000100017>.
13. Awrejcewicz J., Kurpa L., Mazur O. Dynamical instability of laminated plates with external cutout. *International Journal of Non-Linear Mechanics*. 2016. Vol. 81. P. 103–114. <https://doi.org/10.1016/j.ijnonlinmec.2016.01.002>.
14. Awrejcewicz J., Kurpa L., Shmatko T. Analysis of geometrically nonlinear vibrations of functionally graded shallow shells of a complex shape. *Latin American Journal of Solids and Structures*. 2017. Vol. 14. Iss. 9. P. 1648–1668. <https://doi.org/10.1590/1679-78253817>.
15. Kurpa L. V., Shmatko T. V. Investigation of free vibrations and stability of functionally graded three-layer plates by using the R-functions theory and variational methods. *Journal of Mathematical Sciences*. 2020. Vol. 249. No. 3. P. 496–520. <https://doi.org/10.1007/s10958-020-04955-2>.
16. Kurpa L. V., Shmatko T. V. Buckling and free vibration analysis of functionally graded sandwich plates and shallow shells by the Ritz method and the R-functions theory. *Proceedings of the Institution of Mechanical Engineers, Part C: Journal of Mechanical Engineering Science*. 2020. Vol. 235. Iss. 20. P. 4582–4593. <https://doi.org/10.1177/0954406220936304>.
17. Shen H.-S. Functionally graded materials. Nonlinear analysis of plates and shells. USA, Boca Raton: CRC Press, 2011. 280 p. <https://doi.org/10.1201/9781420092578>.
18. Рвачев В. Л. Теория R-функций и некоторые ее приложения. Киев: Наукова думка, 1982. 552 с.
19. Лехницкий С. Г. Анизотропные пластинки. М: Гостехиздат, 1957. 464 с.